

Preventive Medicine Research



PiscoMed Publishing Pte. Ltd.
Address: 73 Upper Paya Lebar Road #07-02B-11
Centro Bianco Singapore 534818
Website: www.piscomed.com
E-mail: contact@piscomed.com



Editorial Board

Editorial Board Member

Dr. Abdul Matin

Majmaah University
Saudi Arabia

Dr. Madhurima Dikshit

Savitribai Phule Pune University
India

Dr. Farzad Firouzi Jahantigh

University of Sistan and Baluchestan
Iran, Islamic Republic of

Dr. Senem Akkoç

Erciyes University
Turkey

Dr. Stavri Chrysostomou

European University Cyprus
Cyprus

Prof. Yousef S. Khader

Jordan University of Science & Technology
Jordan

Dr. Burcu Gul Baykalir

Firat University
Turkey

Prof. Fengqing Hu

Liaoning University
China

Dr. Zarin Zainul

University of Florida
United States

Dr. Purabi Saikia

Central University of Jharkhand
India

Dr. Yuh-Cherng Chai

John Carroll University
United States

Prof. Robert J. Gatchel

The University of Texas at Arlington
United States

Dr. Songül Karakaya

Ankara University
Turkey

Dr. Polychronis Voultsou

Aristotle University of Thessaloniki
Greece

Dr. Rhonda Kristine Spencer-Hwang

Loma Linda University
United States

Dr. Mostafa Norizadeh Tazehkand

Bulent Ecevit University
Turkey

Dr. Djahra Ali Boutlelis

University of El-Oued
Algeria

Dr. Farzaneh Khademi

Shiraz University of Medical Sciences
Iran, Islamic Republic of

Dr. Helio Junji Shimozaoko

University of São Paulo
Brazil

Mrs. Sandra Menard

Universite Laval
Canada

Volume 10 Issue 1·2021
ISSN: 2251-2632

Preventive Medicine Research



Disco Med Publishing



Preventive Medicine Research

<http://ojs.piscomed.com/index.php/PMR>

Contents

Original Articles

- 1 Efficacy and Safety of Paclitaxel and Cisplatin in the Treatment of Advanced Ovarian Cancer by Different Means of Administration**
Datian Fu
- 5 Study on the bacteriostatic effect of Baitouweng on Pseudomonas aeruginosa infection of wounds in rats**
Zhiwei Zhao, Xiaoling Li, Zhuqing Zha, Bo Cui, Yanfeng Li
- 9 A Study on the Effect of IL-17A on Phenotypic Transformation of Fibroblasts in Bleomycin-induced Pulmonary Fibrosis in Mice and Its Mechanism**
Ding Shuqin , Zhao Xiaoyun, Zou Yuechao
- 15 640nm red light irradiation promotes transforming growth factor β induced collagen synthesis by MAPK cell pathway in human dermal fibroblasts**
Yi Bin, Guo Qingxia, He Jun, Han Kejun, Song Nan, Fan Jing
- 24 Under COVID-19 Stress, What We Have Done, How We Are Doing, and What Shall We Do?**
Shun Huang, M.D. Ph.



Efficacy and Safety of Paclitaxel and Cisplatin in the Treatment of Advanced Ovarian Cancer by Different Means of Administration

Datian Fu

Department of Pharmacy, Hainan Women and Children's Medical Center, Haikou 570100, Hainan province, China. E-mail: 4708869717@qq.com

Abstract: In the treatment of advanced ovarian cancer, paclitaxel and cisplatin are administered in different ways. This paper discusses the efficacy and safety of this approach. Methods: Data were searched through literature, and classified discussion was conducted on this basis. The experimental group and the control group were treated in different ways, and the analysis was carried out by way of comparison, so as to explore the therapeutic effect of drug administration route on advanced ovarian cancer patients. Results: After the completion of the statistical survey, the experimental group was compared with the control group by intravenous infusion after using the new administration method. In terms of the results, the intraperitoneal infusion method had a better effect on the treatment of patients. In terms of the data, this method could effectively improve the long-term survival rate of patients. However, in terms of hepatorenal and peripheral neurotoxicity, intraperitoneal perfusion was more toxic. In terms of musculoarthralgia, the type of intraperitoneal perfusion, has a much greater effect on the patient. Conclusions: Intraperitoneal perfusion has positive therapeutic effects in patients with advanced ovarian cancer, but it is more burdensome to the body. Therefore, in the process of use, we should make comprehensive selection according to the specific situation of patients.

Keywords: Paclitaxel; Advanced Ovarian Cancer; Safety Study

1. Introduction

Nowadays, ovarian cancer is the most common cancer in women. According to relevant statistics, the incidence of ovarian cancer has reached the third. Chemotherapy is one of the main treatments in cancer treatment, as is the case in ovarian cancer treatment. In the application of drugs against ovarian cancer, paclitaxel and cisplatin combined administration, which is also the international commonly used treatment means. The usual way to administer the drug is by intravenous infusion. However, in recent years, the new method of drug administration through intraperitoneal perfusion is not uniform in the practical application research due to its short development time, so the outcome and relevant indicators are not uniform. There is no unified report on this method of drug administration at present, and the persuasive power of relevant research reports is mostly limited. In this paper, a meta-analysis was carried out. Conventional intravenous administration was used as a reference control to discuss the efficacy of the new administration, so as to provide theoretical reference for this study. In this paper, a meta-analysis was carried out. Conventional intravenous administration was used as a reference control to discuss the efficacy of the new administration, so as to provide theoretical reference for this study.

2. Materials and methods

2.1 General information

A total of 90 patients with advanced ovarian cancer admitted by a hospital from October 2009 to March 2011 were selected to conduct the study after obtaining the consent of the patients and their families.

2.2 Inclusion criteria

Among the enrolled patients, ovarian cancer was identified first and no other antitumor regimens had been used prior to treatment. Among these patients, treatment with other drugs was required in addition to paclitaxel and cisplatin. Patients who needed other treatments besides chemotherapy were also excluded. At the time of patient selection, a comprehensive review of the patient's condition should be carried out first to ensure that the patient can survive for more than three months and be included in the range. All the patients involved had a full understanding of the treatment plan, agreed to the implementation of the plan, and signed a written explanation.

2.3 Experimental methods

In the treatment, the control group was given conventional intravenous infusion. The experimental group was given the drug by intraperitoneal perfusion. In addition, the treatment plan and symptoms of the patients were consistent.

In the control group, patients were first treated with an intravenous drip of paclitaxel at 135 mg/m². After completion of the injection, cisplatin was administered 24 hours later at 75 mg /m².

In the experimental group, patients were first treated with an intravenous drip of paclitaxel, which was similar to the control group at 135 mg /m². Again, 24 hours later, the patient was intraperitoneally instilled with cisplatin at 100mg/m². Eight days after the completion of this treatment, the patient was given a second intraperitoneal infusion of 60 mg /m² paclitaxel. Before intraperitoneal perfusion operation, patients need to pump ascites to avoid affecting the effect of drugs. The drug was then mixed with warm saline, about 1L of which was used for intraperitoneal perfusion. During intraperitoneal perfusion, patients need to change their position every 30 minutes. The overall length of the infusion is about two hours to ensure that the drug is evenly distributed in the patient's abdominal cavity. In the process of drug administration to patients, appropriate amount of relevant operations, such as hydration, diuresis, etc. Before giving paclitaxel to patients, a certain amount of dexamethasone is injected. In the 6- and 12-hour time periods before the patient starts treatment, patients were given 7.5mg of dexamethasone. Not only that, but diphenhydramine is given half an hour before administration. The dose is 25mg and is given intramuscular. At the same time, cimetidine was injected intravenously with a dosage of 300mg. The goal of this series of measures is to prevent patients from developing allergic reactions to paclitaxel. Blood pressure, heart rate and other data were measured every half an hour after the patients were given paclitaxel. Ondansetron is administered intravenously at 8mg prior to chemotherapy. After medication, the patient's circulatory system and non-hematological adverse reactions were observed. The overall length of treatment was nine weeks, divided into three sessions, each lasting three weeks. After the completion of the treatment, the clinical effect of the patients and the occurrence of adverse reactions, etc. were observed and counted^[1].

2.4 Control indicators

In terms of indexes control, there were short-term effects, long-term survival rate of patients, medication safety, etc. The condition of the patients was examined in a comprehensive way and the clinical efficacy was evaluated. Its standard according to the World Health Organization standard, the patient's diagnosis and treatment effect is divided into four grades, respectively: Complete remission: The patient's lesion was completely eradicated and there was no new disease for more than 4 weeks; Partial remission: The patient's lesion at examination was less than half of the extent before treatment, and there was no evidence of sustained increase; Stable: There is no significant change in the condition before and after treatment; Progression: The disease is further expanded, and even new lesions appear.

In the classification of adverse reactions in patients, the World Health Organization standard is still adopted to classify the symptoms of adverse reactions in patients into grades 0–IV. The adverse reactions of chemotherapy were strong, mainly manifested as leukopenia and significant reduction of hemoglobin. In addition, hair loss, myalgia and arthralgia, renal injury, and peripheral neurotoxicity, are also common adverse reaction symptoms^[2].

3. Statistical results

In the process of carrying out the comparative experiment on these patients, in order to ensure the acquisition of data, all patients in the two groups participating in the experiment should have routine blood examination. The frequency of the examination cycle should be controlled at 1-2 times a week. And the data of patients' liver and kidney functions should also be counted. Therefore, before the course of treatment, the patients need to be led to check the liver and kidney functions. After the treatment, the patients' physical conditions should be checked again comprehensively. The specific statistical data are as follows.

Table 1. Comparison of curative effect between the two groups [%]

Group	Number	Complete remission	Partial remission	Stable	Progression	Effective rate
Control group	45	13 (28.89)	15 (33.33)	12 (26.67)	5 (11.11)	28 (62.22)
Experimental group	45	17 (37.78)	22 (48.89)	5 (11.11)	1 (2.22)	39 (86.87)

In the final results, the quality of body recovery in the experimental group was significantly higher than that in the control group. In addition to the effective rate of patients after the completion of treatment, the adverse reactions of patients and other aspects also need to be counted, and the specific data information is shown below.

Table 2. Adverse reactions in control group were compared [%]

Adverse reactions	I	II	III	IV	Total
Leukopenia	11 (24.44)	8 (17.78)	0 (0.00)	0 (0.00)	19 (42.22)
Hemoglobin reduction	8 (17.78)	5 (11.11)	0 (0.00)	0 (0.00)	13 (28.89)
Thrombocytopenia	2 (4.44)	5 (11.11)	0 (0.00)	0 (0.00)	7 (15.56)
Alopecia	7 (15.56)	5 (11.11)	5 (11.11)	0 (0.00)	17 (37.78)
Myalgia and arthralgia	5 (11.11)	2 (4.44)	3 (6.67)	0 (0.00)	10 (22.22)
Renal injury	3 (6.67)	3 (6.67)	0 (0.00)	0 (0.00)	6 (13.13)
Neurovirulence	4 (8.89)	1 (2.22)	0 (0.00)	0 (0.00)	5 (11.11)
Nausea and vomiting	6 (13.13)	6 (13.13)	1 (2.22)	0 (0.00)	13 (28.89)

Table 3. Adverse reactions in experimental group were compared [%]

Adverse reactions	I	II	III	IV	Total
Leukopenia	23 (51.11)	13 (28.89)	0 (0.00)	0 (0.00)	38 (84.44)
Hemoglobin reduction	16 (35.56)	5 (11.11)	3 (6.67)	2 (4.44)	26 (57.78)
Thrombocytopenia	3 (6.67)	6 (13.13)	2 (4.44)	0 (0.00)	11 (24.44)
Alopecia	12 (26.67)	8 (17.78)	3 (6.67)	2 (4.44)	25 (55.26)
Myalgia and arthralgia	5 (11.11)	2 (4.44)	3 (6.67)	0 (0.00)	10 (22.22)
Renal injury	4 (8.89)	3 (6.67)	3 (6.67)	0 (0.00)	6 (13.13)
Neurovirulence	5 (11.11)	5 (11.11)	7 (15.56)	0 (0.00)	12 (26.67)
Nausea and vomiting	7 (15.56)	6 (13.13)	3 (6.67)	1 (2.22)	17 (37.78)

During the treatment of patients, the incidences of adverse reactions in patients were statistically analyzed. It can be concluded from the above statistical tables that the performance of adverse reactions in patients with intraperitoneal perfusion was significantly reduced.

Table 4. Comparison of survival time cycle of patients

Group	Number	One year	Three years
Control group	45	30 (66.67)	17 (27.78)
Experimental group	45	38 (84.44)	27 (60.00)

After the completion of treatment, the survival time cycle of the patients after treatment was counted. The above table shows that the survival time performance of the patients in the experimental group is better than that of the patients in the control group.

4. Discussion

In gynaecology, ovarian cancer is one of the common tumors. Not only that, when this disease is found, most of

the results are in the late stage. Among the treatment programs in recent years, platinum drugs are the commonly used drugs. On the whole, the therapeutic effect of this drug is relatively obvious^[3]. But the vast majority of patients still die because of drug resistance in their tumors. Paclitaxel is a kind of drug obtained by purifying the bark of purple shirt. In terms of drug classification, it is a semi-synthetic drug^[4]. It is widely used in the treatment of ovarian cancer, but when used alone, its effectiveness is often low.

From the perspective of biological analysis, ovarian cancer is a disease with the nature of abdominal metastasis^[5]. When chemotherapy is administered to patients, intraperitoneal infusion is more direct than traditional intravenous infusion, and can directly affect the tumor at higher concentrations^[6]. And in terms of the experimental data results, this way has less impact on the patients' body and has fewer side effects. In terms of overall therapeutic outcomes, patients survived longer after intraperitoneal perfusion^[7]. It also suggests that this approach is more effective in treating patients than the traditional full injection approach. The drugs acted on the patients' lesions directly through the mucosa without venous blood circulation. In terms of the final therapeutic effect^[8], the results were relatively good. However, from the perspective of adverse reactions in patients, such intraperitoneal perfusion administration significantly increased the incidence of adverse reactions in patients^[9]. In this case, it may be because the drug is absorbed more slowly, or because the dosage is higher. From the perspective of the survival time of patients undergoing implantation, this method is effective^[10], and the way of administration can be adjusted comprehensively according to the physical conditions of patients.

Conclusion: Intraperitoneal perfusion can significantly improve the therapeutic effect of patients, but the incidence of adverse reactions in patients is significantly increased. Therefore, in the process of use, the patient's physical condition should be taken into account, and then it should be promoted vigorously as long as the patient and their condition are acceptable.

References

1. Hu J, Xing J, Chen J, et al. Meta-analysis of the efficacy of paclitaxel combined with cisplatin in the treatment of advanced ovarian cancer by intraperitoneal infusion versus intravenous administration alone (in Chinese). *Journal of North China University of Science and Technology (Health Sciences Edition)* 2020; 22(02): 119–129.
2. Du C. Efficacy and safety evaluation of carboplatin combined with paclitaxel in patients with advanced ovarian cancer and pharmacokinetic study of carboplatin (in Chinese) [Master's thesis]. Tianjin Medical University; 2012.
3. Mu W. Dose exploration and efficacy analysis of carboplatin intraperitoneal infusion chemotherapy for advanced ovarian cancer (in Chinese) [Master's thesis]. Air Force Medical University of PLA (the Fourth Military Medical University); 2018.
4. Chen X, Feng X. Comparison of efficacy of paclitaxel and nedaplatin combined chemotherapy regimens in the treatment of advanced ovarian cancer (in Chinese). *Henan Medical Research* 2015; 24(04): 27–28.
5. Chen Y, Xie R, Liang Y. Clinical effect of paclitaxel combined with cisplatin in the treatment of advanced ovarian cancer and its effect on immune system (in Chinese). *Practical Journal of Clinical Medicine* 2015; 12(04): 134–137.
6. Wu G, Liu L. Efficacy and adverse reactions of different cisplatin methods combined paclitaxel intravenous drip in advanced ovarian cancer. *Chinese Journal of Clinical Oncology and Rehabilitation* 2016; 23(03): 300–302.
7. Hou F. Clinical efficacy and survival rate of neoadjuvant chemotherapy for advanced epithelial ovarian cancer (in Chinese) [Master's thesis]. Lanzhou University; 2020.
8. Zhang Q. Clinical effect of carboplatin combined with paclitaxel in the treatment of advanced epithelial ovarian cancer (in Chinese) [Master's thesis]. Anhui Medical University; 2019.
9. Wang Z. Comparison of efficacy of different administration methods of paclitaxel combined with nedaplatin in the treatment of advanced ovarian cancer (in Chinese). *Shenzhen Journal of Integrated Traditional Chinese and Western Medicine* 2019; 29(18): 157–158.
10. Wang L. Efficacy of different administration of paclitaxel combined with nedaplatin in the treatment of advanced ovarian cancer (in Chinese). *China Continuing Medical Education* 2018; 10(18): 111–112.



Study on the bacteriostatic effect of Baitouweng on Pseudomonas aeruginosa infection of wounds in rats

Zhiwei Zhao^{1,*}, Xiaoling Li², Zhuqing Zha¹, Bo Cui¹, Yanfeng Li¹

1 Department of Hand Microsurgery, Luoyang Orthopedic Hospital of Henan Province (Orthopedic Hospital of Henan Province), Zhengzhou, Henan, 450016, China

2 Health Management Center, Luoyang Orthopedic Hospital of Henan Province (Orthopedic Hospital of Henan Province), Zhengzhou, Henan, 450016, China

Email: zhaozhiwei999@126.com

Abstract: Objective: To analyze the bacteriostatic effect of Baitouweng on Pseudomonas aeruginosa infection of wounds in rats. Methods: Forty Wistar rats were enrolled in the study, among which excisions were made on 30 rats on their upper layer of dorsal skin with an area of 1 cm x 1 cm, the other 10 rats as the control group of sterile wound. Prepared Pseudomonas aeruginosa was applied on the wounds of rats to create infection models. Forty rats were divided into three groups (control group, mafenide group and Baitouweng group) according to different infection methods, and were treated with normal saline, 100g/L mafenide, and 1g/L Baitouweng respectively after 3 hours of injury. The changes in the number of white blood cells in both the wound surface and body of the three groups were observed within one to four days after injury. After that, the changes on the number of both white blood cells and body weight were continuously observed. The survival of the rats in each group was observed on the 14th day after injury. Results: From the observation after injury, compared with the other two groups, rats in control group had more exudation and moist wounds, and the activities of rats decreased while the death rate increased. On the 3rd day after injury, the number of white blood cells in each group decreased, and the number of Pseudomonas aeruginosa in the control group was significantly higher than that in the other two groups ($P < 0.01$). The rats in the sterile wound control group did not die and continued to gain weight. After 14 days, the survival number of rats in control group was significantly less than that in mafenide group and Baitouweng group ($P < 0.05$). Conclusion: Baitouweng has obvious bacteriostatic and virus-killing effects on Pseudomonas aeruginosa infection of wounds in Wistar rats, reducing mortality rate effectively, and has practical value as well as development and application prospects.

Keywords: Baitouweng; Pseudomonas Aeruginosa; Wound Infection

1. Foreword

Pseudomonas aeruginosa, also known as pseudomonas, often occurs in nature, such as soil, and wet parts of the body, such as human intestinal tract. Pseudomonas aeruginosa has low nutritional requirements but with strong drug resistance and has great harm, especially to the middle-aged, the elderly and infants who has low immunity. This kind of bacterium is easy to cause disease, such as septicemia, and acute gastroenteritis. Therefore, early prevention, early detection and early treatment are the main treatment principle, and the inhibition of the bacteria has become a crucial issue to overcome. Baitouweng was first recorded in Shennong's Herbal Classic of Materia Medica and had been widely

used in ancient Chinese medicine. With the development of modern medical science and technology, it has been found that Baitouweng has clear bacteriostatic effect on pathogens such as *Escherichia coli* and *Paratyphoid Bacillus*, and the extracted effective components are protoanemonin and anemonin. Safe drug usage has become a broad consensus in the medical field nowadays. In this case, exploring antibacterial drugs from traditional Chinese herbal medicines has become a hot research topic. This study deeply explores the antibacterial effect of Baitouweng on *Pseudomonas aeruginosa*. Details are reported as the following contents^[1].

2. Materials and methods

2.1 Animal origin, strains tested and experimental drugs

Wistar rats were all male and introduced from animal experiment center of a medical university. Their body weight ranged from 200 g to 250 g. *Pseudomonas aeruginosa* was provided by microbiology laboratory. Baitouweng is purchased from the Chinese medicine pharmacy in our hospital.

2.2 Preparation and purification of protoanemonin

Baitouweng weighing 150g was put into a round bottom flask, and was mixed with distilled water at a ratio of 1:10. After soaking for one hour and heating for one hour, the dregs were filtered with gauze. Then, eight times and six times of distilled water were poured into the dregs to repeat soaking and heating operation. The solution obtained from the above three treatments was concentrated and purified, so that the concentration of the liquid was stabilized at 1g/L and stored in the freezer.

2.3 Preparation of *Pseudomonas aeruginosa* suspension

Pseudomonas aeruginosa in culture medium was separated through centrifugal separation, with 2000r/min centrifugal rate and 15min duration. It was washed repeatedly with normal saline and then re-suspended to a concentration of 1×10^8 CFU/ml. After incubation at 37°C for 24 hours, the number of colonies was identified by blood cell counting plate.

2.4 Detection of antibacterial activity

Pseudomonas aeruginosa was cultivated on the culture medium, and solution and distilled water of Baitouweng were injected respectively as control group. After being cultivated at 37°C for 24 hours, the results showed that Baitouweng had a strong inhibitory effect on *Pseudomonas aeruginosa*.

2.5 Establish infection models

One day before injury, 30 rats were selected, and the other 10 used as control group of sterile wound. After anesthesia, fixation and hair removal, the upper layer of the skin was cut with a wound area of 1cm×1cm by a scalpel. Prepared *Pseudomonas aeruginosa* bacterial solution was smeared on the wound of rats to establish infection models.

2.6 Groups

Randomized sampling and different nursing methods were used to divide rats into three groups, which are control group, mafenide group and Baitouweng group. A total of 40 rats in the three groups were kept in the same environment, where was clean and dry with 25°C of constant temperature. The changes of the number of white blood cells in the wound and body of the three groups were observed within one to four days after injury. Then the changes of white blood cells and body weight were continuously observed, and the survival of the rats in each group was observed on the 14th day after injury^[2].

2.7 Statistical analysis

All the collected prescription-related data in this paper are processed and analyzed through SPSS20.0 software, saving the cost of manual calculation and improving the accuracy and efficiency of calculation. The unit of measurement

is expressed by ($\bar{x}\pm s$) with t test. If $P<0.05$, it is statistically significant.

3. Results

3.1 Changes of wound surface

From the observation after injury, compared with the other two groups, the wounds in the control group had more secretions and moist wounds. In addition, the activities of rats in the control group decreased and the death toll continued to increase.

3.2 Quantification of *Pseudomonas aeruginosa*

After data collection and statistics, it was found that *Pseudomonas aeruginosa* in the control group was significantly higher than that in the other two groups. See Table 1 for detailed data.

Table 1. Quantification of *Pseudomonas aeruginosa* in the scab of rats in each group on the third post-injury day

groups	Before injury	Different quantitative levels of bacteria		
		< 103	103~105	> 105
Control group	10	0	0	10
Mafenide group	10	5	5	0
Baitouweng group	10	10	0	0

3.3 Survival rate and weight test

After data collection and analyzing, it was found that on the 3rd post-injury day, the death number of rats reached five in control group, followed by mafenide group, two death rats, and Baitouweng group, one rat. By the 14th day, the survival rate of rats in control group was only 30%, and the other two groups remained unchanged. On the 6th post-injury day, the weight of rats decreased significantly in the control group compared with other two groups. Besides, there was little difference between the mafenide group and Baitouweng group. See Table 2 for details.

Table 2. White blood cells on the third post-injury day and weight of rats on the sixth post-injury day

R a t s number	White blood cell count ($\times 10^9/l$)			Weight (g)		
	control group	Mafenide group	Baitouweng group	control group	Mafenide group	Baitouweng group
1	—	3.95	3.9	—	19.1	20.9
2	—	5.65	4.25		18.3	19.5
3	2.95	4.10	3.1	16.9	20.3	18.4
4	—	4.3	4.25	—	20.8	19.0
5	3.65	—	4.2	16.7	—	18.8
6	3.35	3.75	4.9	16	19.7	19.8
7	—	3.95	3.9	—	19.4	19.1
8	3.5	4.05	—	—	19.8	—
9	3.45	4.25	3.6	—	20.6	20.4
10	—	—	5.95	—	—	19.6
$\bar{x}\pm s$	3.38±0.26	4.44±0.79	4.01±0.53	16.53±0.47	19.73±0.77	19.49±0.84

Notes: "—" suggests that the rat died.

4. Discussion

As one of the representatives of pathogenic bacteria in current clinical treatment, *Pseudomonas aeruginosa*, widely

distributing in nature, its drug resistance is increasing year by year, while its morbidity and mortality are also high, being a tricky issue in medical treatment. Even in hospitals, patients can be infected with *Pseudomonas aeruginosa*, because the pathogen mostly grows in humid environment. It is surveyed that the infection rate of *Pseudomonas aeruginosa* in hospitals is about 10% to 15% around the world. The isolation rate of *Pseudomonas aeruginosa* in the diagnosis of acquired pneumonia is as high as 20.9% in China, which is a very serious situation. Under such situation that there are many drug-resistant pathogenic bacteria strains at present, how to realize symptomatic prevention and treatment and maximize the effectiveness of antibacterial drugs in the treatment process has become an urgent issue for each clinician^[3].

Baitouweng belongs to a kind of Chinese herbal medicine, which has been used to kill bacteria and insects since ancient times. In recent years, with the continuous advancement of the medical research and analysis on the chemical constituents and pharmacological effects, Baitouweng has drawn people's attention with a brand-new understanding. In modern research, Baitouweng has clear inhibitory effect on known strains such as *Shigella dysenteriae* and *Bacillus subtilis*. Compared with western medicine, Baitouweng will not produce too many toxic and side effects, especially in the case of antibiotic abuse.

Mafenide is recognized as an effective antibacterial drug against *Pseudomonas aeruginosa* in present clinical treatment. However, with the long-term use of the drug, it is inevitable that the therapeutic effect will be reduced due to the increase of bacterial drug resistance. Therefore, it is necessary to find new effective inhibitory components to alleviate this phenomenon. In this study, mafenide group and Baitouweng group were compared to on the one hand, verify the antibacterial effect, on the other hand, to verify whether the extract from Baitouweng can further replace mafenide as an antibacterial medicine for wound. From the wound infection, the wounds of the two groups of rats are basically the same, both of which are scabbed, dry and have little secretion. From the quantitative point of view of *Pseudomonas aeruginosa*, the antibacterial effect of Baitouweng group is better. It is because the protoanemonin and anemonin in Baitouweng can destroy the cell membrane and cell wall of *Pseudomonas aeruginosa* to achieve the bactericidal effect. At the same time, it will enhance the antibacterial effect with the extension of time. From the other indicators, there is little difference between the weight of the two groups and the number of white blood cells. The mortality rate of rats in the Baitouweng group will be lower, which indicates that it is feasible to use Baitouweng as an anti-*Pseudomonas aeruginosa* drug. However, whether it is functional in human body remains to be confirmed.

In summary, Baitouweng has obvious bacteriostatic and virus-killing effects on *Pseudomonas aeruginosa* infected wounds on Wistar rats. It effectively reduces rats' mortality rate, and has practical value and development and application prospects.

References

1. Ren H, Han C, Zhang R, et al. The antibacterial effect of cecropin B on *Pseudomonas aeruginosa* infection of wounds in mice. *Chinese Journal of Burns* 2006; 22(6): 445-447.
2. Wang L, Li X, Wang D, et al. Antibacterial effect of antimicrobial peptide from skin secretions of *Andrias davidianus* on the wound of *Pseudomonas aeruginosa* infection in mice. *West China Journal of Pharmaceutical Sciences* 2011; 26(4): 336-339.
3. Wang L, Tao X, Ouyang J, et al. Bacteriostasis in Vitro Effect of Baitouweng Decoction on *Shigella Dysenteriae*. *Information on Traditional Chinese Medicine* 2020; 37(05): 49-53.



A Study on the Effect of IL-17A on Phenotypic Transformation of Fibroblasts in Bleomycin-induced Pulmonary Fibrosis in Mice and Its Mechanism

Ding Shuqin¹, Zhao Xiaoyun^{2*}, Zou Yuechao²

1. NO. 943 Hospital of PLA Joint Logistic Support Force, Wuwei City 733000, Gansu Province.

2. Hexi University, Zhangye City 734000, Gansu Province.

Corresponding author: Zhao Xiaoyun, male, 1980-, associate professor, Teacher from Medical College of Hexi University; Research orientation: Basic medical research.

Fund: Hexi University 2018 Principal's Fund Project of Scientific Research Innovation and Application; No: XZ2018016

Journal: Preventive Medicine Research

Abstract: Objective: In this study, lung fibroblasts were cultured and identified in mice lung fiber model with bleomycin. Under the induction of IL-17A, lung fibroblasts were gradually transformed into myofibroblasts in pulmonary fibrosis, and the specific induction effect of IL-17A in pulmonary fibrosis was analyzed, which could provide ideas for the prevention and treatment of clinical pulmonary fibrosis. Methods: To investigate the transcriptional expression of bleomycin-induced fractional pulmonary fibrosis in different pulmonary fibrosis processes. The 14-day mice model was taken as the research object, and the pulmonary fibrosis model was established by induction of myogenesis. After 14 days of modeling, lung tissue was removed, and after centrifugation and repeated adherent treatment, lung fibroblasts could be cultured at the origin. After three generations of culture, the morphological changes of lung fibroblasts could be observed under a microscope. Indirect immunofluorescence was used to establish the expression of vimentin, and IL-17 was used to stimulate primary cultured lung fibroblasts to detect the expression and specific localization of α -SMA in cells. Western blotting was used to stimulate the expression of lung fibroblast protein by IL-17A at different time points. Results: The typical characteristics of primary culture lung fibroblasts were obtained. After purification and culture, lung fibroblasts were obtained in morphology. The morphology of the 3rd and 4th generation cells was relatively uniform, showing long carboxyform. 1-2 nucleoli can be observed by microscope, which have distinct cell boundary and are lined up like fish schools. The results of indirect immunofluorescence showed that the vimentin staining in the third generation cells was positive, and the plasma was dark red. There were collagenous fibrous septa between the cells, which might make them develop into lung fibroblasts. A-SMA immunofluorescence results showed that in the absence of IL-17A induction, A-SMA signal was relatively weak in the lung fibroblasts of the control group and was in the cytoplasm, while after IL-17A induction, A-SMA signal was stronger in the lung fibroblasts of mice and the whole cells presented spindle structure. Western blotting showed that lung fibroblasts were stimulated by IL-17 in the 0h group. Compared with the 1h, 2h, and 4h groups, the expression of A-SMA in lung fibroblasts was significantly increased in the 1h, 2h, and 4h groups. The fibroblasts were very low in the 2h and 4h groups. There was no significant difference in the ex-

pression of AS MA signal. Compared with 0h, protein contents of p-IKB-a and p-p65 were higher in lung fibroblasts at 1h, 2h and 4h. Protein expressions of Acti, 1P6, IKB-a and P65 were different in lung fibroblasts, but there was no significant difference. However, there was no significant statistical difference in the expression of these proteins in lung fibroblasts at different times. Conclusion: By differential centrifugation and repeated adhesion, bleomycin-induced lung fibroblasts can be isolated and purified, and more cell production can be obtained. The staining vimentin was strongly positive after identification by indirect immunofluorescence. The stimulation of IL-17A could gradually transform non-fibroblasts into myofibroblasts and play an important role in pulmonary fibrosis. Therefore, through experimental studies, it was found that IL-17A stimulated F-kB signal and then increased the expression of P-IKB-a and P-P65 proteins, and transformed non-phosphorylated proteins into phosphorylated proteins, thus transforming lung fibroblasts into myofibroblasts and playing a role in pulmonary fibrosis.

Key words: IL-17A; Pulmonary Fibrosis; Fibroblasts; Transformation

1. Introduction

Interstitial pulmonary disease is a group of pulmonary diseases with varying degrees of fibrosis and inflammation, and is also a disease of idiopathic pulmonary fibrosis. The clinical manifestations are dyspnea, dry cough and other symptoms, and the imaging manifestations are diffuse interstitial and parenchymal injury. The mortality and morbidity of this disease are high. However, there is no effective treatment for this disease and the cure rate is relatively low. Therefore, the focus of current clinical research is to explore the pathogenesis of pulmonary fibrosis and find effective therapeutic drugs^[1].

2. Research materials and methods

2.1 Animal sample sources

In this study, a total of 20 SPF male mice with an average age of 7 weeks and a weight of 20 grams were selected and purchased from an animal experiment center of a university. During the feeding process, the temperature and humidity of the mice were required to be kept at 20°C and 65% to ensure free water intake.

2.2 Reagents and instruments

The experimental materials used in this experimental study included IL-17A reagent, bleomycin powder, fetal bovine serum or anti-mouse antibodies, trypsin, 3% barbital solution, penicillin, streptomycin, recombinant mice, RIPA, BSA, PMSF, goat anti-rabbit IGG-HRP, and P-mouth DF membrane. The instruments used in the research include animal laboratory instruments, such as scalpel, gauze, transcendence table, alcohol lamp, scales, centrifuge, water bath, carbon dioxide incubator, etc.

2.3 Research Methods

How to select research objects? For the previous studies on the expression of IL-17RAMRNA in the lung tissues of PF mice induced by bleomycin in different stages of PF formation, the model mice on the 14th day could be selected as the research objects. The method and process of making mice PF model induced by bleomycin were consistent with previous experiments.

When drawing concrete materials, the culture bottle was wrapped with gelatin, and after one night culture, the gelatin was taken out. Meanwhile, 2 ml of the culture solution was poured into the culture bottle, and then place the culture bottle on super worktable and take out the lung tissue of the mice by dissecting the mice. In dealing with the specific operation, it can adopt routine cervical dislocation method to avoid death. Then it shall use ethanol for surface sterilization. The skin on the chest of mice could be disinfected with iodine first and then cleaned with alcohol. The left hand can pinch the neck and back of the mouse to expose the skin of the chest of the mouse, while the right hand

can cut the skin of the mouse. After using alcohol disinfection, it can cut the ribs along the lower end of the sternum of the mice and cut the sternum transversally in the middle of the incision of the mice to take out the lung tissue, and then put the tissue in the double antibody culture flask. The primary lung tissue of mice was cultured, and the lung tissue was cut into multiple lung lobes through PPS buffer solution, and the excess blood vessels and bronchus at the hilum of the mice were subtracted, and the pleura was removed[2]. Then it shall transfer the lung tissue into the culture bottle containing penicillin. After repeated PPS cleaning, lung tissue fibers can be cut to a cubic millimeter size tissue block. And then double anti PBS suspension was used. After the tissue naturally sank, it shall abandon supernatant for three times repeatedly, until the supernatant keep clear. Then use 0.1% of the pancreatic enzyme to clean the tissue and add 1 ml of 0.1% trypsin for each mouse. After being digested at 37°C for 20 minutes, most of the tissues can be digested into suspension. After adding the same amount of digestive solution, 10% DMEM containing FBS can be added to stop digestion after a period of time. After being beaten evenly, the cells are filtered to obtain cellular blood centrifugation. And then add 35ml of DMEM to the sediment. After 5 minutes' centrifugation, collect the supernatant and sediment respectively. Among them, LF is mainly distributed in the supernatant, and a few are epithelial cells. After centrifugation, the supernatant was discarded. Then use an incubator containing 5% carbon dioxide to culture the tissue at 37°C for 40 minutes, and remove the unattached cells in time, among which the attached cells were mainly LF. 0.5ml of culture solution was replaced for overnight culture, and 2ml of culture solution was added on the second day for further culture. The sediments are epithelial cells, and a few contains LF. The sediments can be removed by centrifugation for 5 minutes, and then add it into 10%FBS of DMEM culture solution. After resuspend the sediments, transfer it into a 25ml culture bottle. Then use the same method to continue culture, the most unattached cells are epithelial cells. After absorption and discarding, abandon the supernatant by centrifugation at low temperatures and resuspend the sediments in the culture bottle to remove unattached cells by repeatedly beating two or three times, among which LF are the attached cells. After adding culture solution into culture bottle for overnight culture, the structure and growth of the cells can be observed by telescope. At the same time, the survival of cells was determined by staining. After three days of isolation and purification, the cells were close to fusion state, and then they were connected into a network structure. When the cells reached 90% fusion, the subculture could be carried out according to a ratio of 1:2.

2.4 Observation Indicators

First, identify the lung fibroblasts of the mice. The cell slides of primary culture and third-generation culture can be selected and fixed with 4% paraformaldehyde for indirect fluorescence immunochemical staining of vimentin. Second, observe the structural changes of lung fibroblasts, and then observe LF form after cell culture with an inverted microscope. Third, after IL-17A stimulation, observe the expression of A-SMA signal and its specific localization. Fourth, observe phenotypic changes under the IL-17A simulation at different time points and then analyze transcriptional indexes and expression of transcriptional suppressor genes and activation of target genes^[3].

3. Research Results

First, observe the morphology of lung fibroblasts(see Figure 1). When observing the structure of LF in vitro culture through inverted microscope, it can be found that in 30 minutes' meta-generation culture, the cells can grow adhere to the wall, but part of the hematopoietic cells may suspend in the culture solution. After 24 hours of culture to obtain new culture solution, remove suspending cells to improve the growth number of the attached cells, which are round or polygonal in shape. Such cells are mainly transparent and have relatively big cell nucleus and 2-3 nucleoli, which were in line with the structural morphological characteristics of Fb. After further culture for 36~48 hours, the cells entered the logarithmic phase, and the FB cells increased and were arranged radially or helically. After 72 hours of culture, most of the cells were found to be spindle-shaped, accompanied by some quasi-circular or circular structures. It can be observed through the microscope that local cells mainly grew in scattered forms. After one week of culture, attached cells showed long fusiform and abundant cytoplasm. 1~2 nucleoli and relatively clear cell boundaries could be observed through the

microscope, which arranged like fish schools.

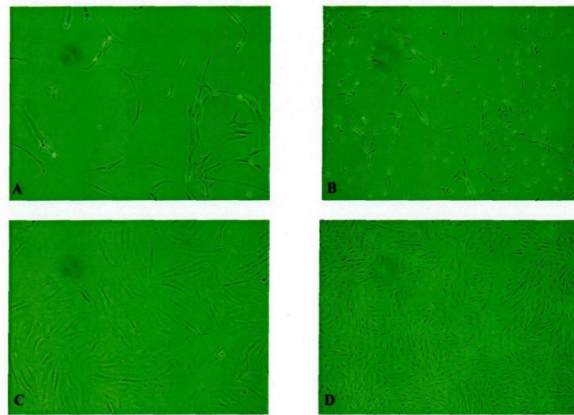


Figure 1. Morphology of lung fibroblasts

Identify lung fibroblasts (see Figure 2). After the observation of the vimentin cultured in the third generation by laser confocal microscope, since the protein staining of the vimentin cultured in the third generation showed strong positive with dark red cytoplasm and collagenous fibrous septa between the cells, it could be confirmed as LF.

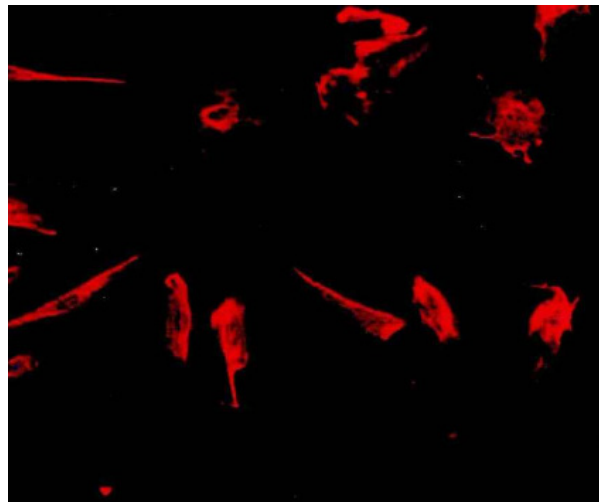


Figure 2. Identification of lung fibroblasts

According to the results of A-SMA immunofluorescence (see Figure 3), it was found that after the stimulation of IL-17A, the LF cells in childhood had a strong S-AM fluorescence signal, which was in the plasma envelope. After the stimulation of IL-17A, the mice had a strong A-SMA fluorescence signal, and the whole cells presented a spindle state. After the stimulation of IL-17A, the expression of different proteins in lung fibroblasts could be detected by using Western blotting at different time points, including p65, P-p65, IKB-a, p-IKB-a and ACT1.

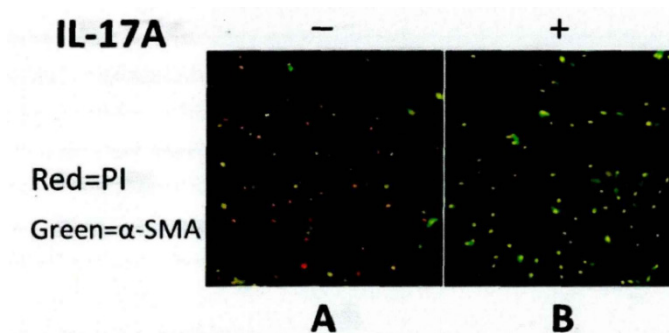


Figure 3. The results of A-SMA immunofluorescence

First, select LF with good growth condition, adjust its density to a certain range and inoculate it in the new solution, and the cells will grow adherently the next day. IL-17A was added to the serum-free culture solution after 24 hours, and then cells were collected after 0, 1, 2, and 4 hours respectively, and the cells were quantified by lysis. Western blotting assay was used to detect the expression of different proteins, including α -SMA, ACTL, p65, P-p65, I κ B- α , and P-I κ B- α (see Table 1). The results showed that the expression of α -SMA in LF of the 0 h group was weak. After 7 hours of IL-17A stimulation, the expression of α -SMA in LF in 1 hour, 2 hours and 4 hours was higher than that in 0h mice group. Compared with that in 1-hour group, the expression of α -SMA in 2h and 4h group was increasing. There was no significant difference in the expression of A-SMA in LF between the 2h and 4h group. In other words, after LF was induced by IL-17A, A-SMAs increased in 1h, and reached the peak in 2h, and then maintained high expression in 4h. The results of optical density and image table scanning showed that the protein expression levels of P-I κ B- α and P-p65 in LF cells at 1h, 2h, and 4h after IL-17A stimulation were significantly higher than those at 0h. The protein expression of p-I κ B-A and p-p65 was not significantly different between LF in 2h and 4h. After the stimulation of IL-17A, the protein expression of P65 and P-I κ B- α in mouse LF was higher at different time points, and there was no significant difference in the expression of the two proteins at different time points. Once again, the expression of P65 and p-I κ B-A proteins in mouse LF cells was not affected by IL-17A induction. However, after the stimulation of IL-17A, the phosphorylation of I κ B- α and P65 protein reached the peak within 1 hour. The expression was lower in 2 hours group and higher in 4 hours group than that in 0 hour group. In addition, there was no significant change in the expression of Actl protein in LF cells after IL-17A stimulation at different time points, and the expression of this protein was consistently low^[4].

Table 1. Expression of α -SMA, ACTl, p65, P-p65, I κ B-A and P-I κ B-a proteins at different times

	N	0h	1h	2h	4h
α -SMA	20	0.290±0.007	0.445±0.010*	0.706±0.014* ^Δ	0.700±0.016* ^Δ
P-p65	20	0.248±0.009	0.570±0.011*	0.490±0.024* ^Δ	0.484±0.025* ^Δ
p65	20	0.944±0.015	0.950±0.016	0.943±0.017	0.942±0.015
P-I κ B- α	20	0.368±0.012	0.718±0.013*	0.466±0.020* ^Δ	0.461±0.020* ^Δ
I κ B- α	20	0.283±0.013	0.286±0.012	0.282±0.012	0.281±0.014
Act1	20	0.265±0.044	0.261±0.018	0.266±0.023	0.275±0.021

4. Discussion and conclusion

In vitro and in vivo studies have shown that GF- β 1 plays an important role in the transition from Fb to MFb. According to studies, it can promote the transition of Fb from MFb through smads signal, but the smads signal pathway is not the only one involved in the transition from Fb to MFb. Hashimoto showed that GF- β 1 could also promote MFb transformation through JNK. Studies have shown that both TGF- β 1 and MAPK signal pathways can participate in the regulation and expression of α -SMA in lung fibroblasts. MAPK signal pathway is composed of ERk and P38MAPK, and other cytokines can utilize this signal pathway and participate in the phenotypic transformation process from Fb to MFb. In addition, the MAPK pathway can also be activated by mechanical tension to promote the regulation of non-tissue fibrosis. IL-17A plays an important role in the formation of PF, which is influenced by a variety of cytokines. Therefore, the following speculation can be proposed: IL-17A can participate in the formation of PF during the transformation from FB to MFB. In this study, the Western blotting experiment showed that IL-17A played an important role in promoting the formation of PF, and its A-SMA indirect immunofluorescence experiment was consistent with previous conclusions. It can be speculated that IL-17A can increase the protein expressions of P-p65 and P-I κ B- α in cells through the activation of NF-KB signal pathway, and transform non-phosphorylated proteins into phosphorylated proteins, thus promoting the

gradual transformation of fibroblasts into integrated fibroblasts, and finally forming pulmonary fibrosis.

References

1. Du X, Yan Y. Clinical significance of changes of serum cystatin C and β 2 microglobulin in patients with type 2 diabetic nephropathy before and after treatment (in Chinese). *Special Health* 2020; 000(001): 80–81. doi: 10.3969/j.issn.2095-6851.2020.01.106.
2. Hua X, Wang C. A study on ERK5 inhibitor in promoting autophagy of lung fibroblasts and its role in pulmonary fibrosis in mice (in Chinese). *International Journal of Respiration* 2020; 40(24): 1849–1855. doi: 10.3760/cma.j.cn131368-20200319-00187.
3. Zhang X, Song G, Nian X, et al. Effect of interleukin-17 blocking on bleomycin-induced pulmonary fibrosis and Fas/FasL expression in lung tissue in mice (in Chinese). *Journal of Nanjing Medical University (Natural Sciences)* 2017; 037(005): 584–587.
4. Zhang H. IL-17A induced EMT response in experimental colitis and intestinal fibrosis (Dissertation). China Medical University 2019.



640nm red light irradiation promotes transforming growth factor β induced collagen synthesis by MAPK cell pathway in human dermal fibroblasts

Yi Bin ¹, Guo Qingxia ¹, He Jun ¹, Han Kejun ¹, Song Nan ¹*, Fan Jing ²*

1. Beijing ChuangPhotoelectric Medical Technology Co., Ltd., Beijing 100176; 2. Beijing Qintang Biotechnology Co., Ltd., Beijing 100730

Abstract: Purpose Transforming growth factor β is a key regulatory factor of collagen expression in human fibroblasts. 640nm red light can regulate the proliferation and transforming growth factor β expression of fibroblasts. Mitogen-activated protein kinase signaling pathway is involved in many physiological processes, such as cell proliferation, differentiation, and apoptosis. The study aims to investigate the effect of 640nm red light irradiation on collagen expression in fibroblasts and the specific regulatory mechanism of mitogen-activated protein kinase signaling pathway. Methods The cells were treated with 640 nm red light for different irradiation time. The effect of real-time fluorescence quantitative PCR detected gene expression of transforming growth factor β and collagen. The specific regulation mechanism of mitogen-activated protein kinase signaling pathway was assessed by western blotting. Results Red light irradiation at 640nm significantly up-regulated mRNA expression of transforming growth factor β , which promoted the expression of collagen mRNA. 640nm red light activated the protein phosphorylation of ERK and inhibited the phosphorylation level of P38 in mitogen-activated protein kinase signaling pathway, which promoting the proliferation of fibroblasts and the gene expression of collagen. Conclusion: 640nm red light irradiation can promote collagen synthesis through cell proliferation and the expression of transforming growth factor β and collagen. Phosphorylation of ERK and P38 promoted cell proliferation and up-regulates mRNA level of collagen.

Key words: Red Light Irradiation; Human Fibroblasts; Stretch Marks; Transforming Growth Factor β ; Collagen; Mitogen-Activated Protein Kinase Pathway

1 Introduction

Skin is the largest organ of human body, which not only plays a role in protecting the body and regulating body temperature, but also affects people's appearance^[1, 2]. Stretch marks are linear dermal skin lesions that occur during pregnancy^[3]. Stretch marks firstly appear as dark red or purplish streaks, then become de-pigmented, flabby, shriveled, and finally stabilize as a white or silver wrinkled paper appearance^[4]. Stretch marks are not harmful to physical health, but they cause great damage to the appearance of patients. Stretch marks bring great mental pressure and psychological burden to patients, and affect their quality of life^[5]. Therefore, the treatment of stretch marks has been widely concerned and constantly explored.

The treatment of stretch marks mainly include drug therapy, laser therapy, minimally invasive surgery, red light therapy and so on^[6]. However, there is no clear and unified treatment method. Recent years, more and more studies on the treatment of stretch marks have focused on red light therapy^[7]. The wavelength of red light is generally between

600nm-700nm, and red light treatment mainly relies on photochemical action rather than energy action^[8]. Presently, red light therapy is used in anti-inflammation^[9], accelerating tissue repair^[10], promoting fracture healing^[11], and reducing scar^[12]. 640nm is a small wavelength of red light, which is mainly used in the field of skin therapy^[13]. Stretch marks are the marks left behind by skin lesions, and the effect of 640nm red light on stretch marks is unclear.

Although the causes of stretch marks are not well understood, the main believed causes of stretch marks are changes in skin tension and hormonal changes during pregnancy^[14]. During pregnancy, the skin will be gradually stretched with the expansion of subcutaneous tissues such as fat and muscle^[15]. Expansion of tissues results in dermal connective tissue damage, collagen fibers and elastic fibers broken, which induced the weakened extensibility and elasticity of the lesions, resulting in striped skin damage^[16]. Hormone receptor expression and hormone levels also change dramatically during pregnancy. The surge of glucocorticoid can inhibit the activity and proliferation of fibroblasts, and reduce the synthesis of elastic fibers and collagen of fibroblasts, thus impeding the complete repair of the damaged connective tissue in the dermis^[17, 18]. The stationary myofibroblasts of stretch marks are unable to synthesize collagen and elastin^[19]. The regulation of collagen by fibroblasts is related to the differentiation status of cells. Mitogen-activated protein kinase (MAPK) signaling pathway is related to a variety of cell functions, and can be involved in a variety of physiological processes such as cell movement, apoptosis, growth and proliferation^[20-22]. MAPK pathway has three levels of signaling: MAPK, MAPK kinase (MEK or MKK), and the kinase of MAPK kinase (MEKK or MKKK). Three kinases can be activated to regulate a variety of physiological/pathological effects of cells.

The MAPK pathway has four main branching routes: the extracellular signal-regulated kinase (ERK) pathway^[23], the c-Jun N-terminal kinase (JNK)/stress-activated protein (SAPK) pathway, the p38 MAPK pathway^[24] and the ERK5/mitogen-activated protein kinase (BMK1) pathway^[25]. Specially, JNK and p38 have similar functions, which related to inflammation, apoptosis and growth^[26]. ERK pathway mainly channels the growth and differentiation of cells, and its upstream signal is the famous Ras/Raf protein. ERK protein include ERK1 (P44) and ERK2 (P42), which are essential for the transmission of signals from surface receptors to the nucleus. Each signal pathway is highly specific and has independent functions^[27, 28]. To some extent, several signal pathways are cross-linked. Stretch marks are associated with the differentiation of fibroblasts^[29]. The repair of stretch marks was accompanied by the proliferation and differentiation of dermal fibroblasts. The 640nm red light could promote the repair of stretch marks. The regulatory mechanism of 640nm red light on collagen and the role of MAPK signaling pathway is still unclear. The study aims to explore whether 640nm red light regulates collagen expression by affecting MAPK signaling pathway, which to induce the the repair of stretch marks.

2 Materials and methods

2.1 Experimental materials

2.1.1 Cells: human dermal fibroblasts (Sciencel)

2.1.2 Reagents: Fibroblast culture media (Novozyme Bio-Tech Co Ltd., R401-01), trypsin EDTA (Solibol, T1300), Trizol (Thermofisher, 15596026), Reverse Transcribing Kit (Thermofisher, 4368813), Absolute Blue qPCR Mix, SYBR Green, Low Rox (Thermofisher, AB4323A), MAPK Family Antibody Sampler Kit (CST, 9926), Phospho-MAPK Family Antibody Sampler Kit (CST, 9910T), anti- β -actin murine monoclonal Antibody (Sigma, A5316), HRP-conjugated sheep anti-mouse second Antibody (Jackson, 515-005-003), HRP-conjugated sheep anti-rabbit second Antibody (Jackson, 111-005-003), Ripa Lysis and Extraction Buffer (Thermo, 89901), Pierce™ BCA Protein Assay Kit (Thermo, 23225), Pierce™ Fast Western Blot Kit, ECL Substrate (Thermo, 23500), ERK inhibitor (Selleck, S1013), JNK inhibitor (Selleck, S7794), P38 inhibitor (Selleck, S1076), AX-II X-ray photography cassette (Yuehua, 60015797), medical X-ray film (Carestream, X001), other chemical reagents are Sino pharmaceuticals.

2.1.3 Experimental materials: 6-well plate (Corning), 96-well plate (Corning), PCR eight-tube.

2.1.4 Experimental apparatus: carbon dioxide incubator (SANYO, MC0-15 ac), biological safety cabinet (haier,

HR40 - IIA2), centrifuge (Beijing times north, centrifuge, D75-2 b), enzyme standard instrument (Thermo Fisher, MULTISKAN FC), microscope (aurora borealis puca technology co., LTD., IM200), PCR instrument (biological technology co., LTD., Beijing dongsheng innovation ETC811), fluorescence quantitative PCR (ABI, Step One).

1.2 Methods

1.2.1 Cell culture: the resuscitated cells were gently shaken and melted in a water bath at 37°C and transferred into a centrifuge tube containing 10ml dulbecco's modified eagle medium (DMEM); Centrifuge at 1000rpm /min for 5min, pour out the supernatant, add medium to the centrifuge tube and suspend it, then transfer it to the culture flask; The cells were proliferated to 80% density for passage.

1.2.2 Cell irradiation: After the cells were cultured to the third generation, the experiment groups were irradiated by 640nm red light for different irradiation time (30 min, 60 min, 120 min) respectively. Meanwhile, the non-irradiation group was set for comparison. After irradiation for different times, the cells were cultured and collected at 12 h, 24 h, 36 h, 48 h, 60 h and 72 h for detection of cell activity, growth status and gene expression level.

1.2.3 Fluorescence staining: Cell slides were dipped and washed with PBS for 3 times, 3min/ time; It was fixed with 4% paraformaldehyde for 15min, then washed with PBS for 3 times, 3min/ time; 0.5% TritonX-100 penetration for 20min, PBS washed for 3 times, 3min/ time; The goat serum was sealed at room temperature for 30min, and the primary antibodies were incubated overnight at 4°C. PBST was washed for 3 times, 3min/ time. Fluorescence labeled sheep anti-rabbit labeled IgG was incubated for 1h. PBST was washed for 3 times, 3min/ time. DAPI was used to stain the core and seal the film, and the images were observed and collected.

1.2.4 Preparation of cDNA: Cells were collected to mix with 500uLTRIZOL, and then lysed for 5min; Add 100ul chloroform, blowing and mixing with the tip of a gun at room temperature for 10min, and centrifuge at 12000rpm at 4°C for 15min. Transfer the supernatant to a new tube, add isopropanol of equal volume, blow and mix, stand for 10min at room temperature, and centrifuge for 5min at 12000rpm at 4°C. The supernatant was discarded and added with 1mL of anhydrous ethanol, rinsed and precipitated gently, and centrifuged at 6000rpm at 4°C for 5min. The supernatant was dried at room temperature, then 30uL water was added to dissolve RNA and stored at -80°C. RNA was transcribed into cDNA according to the reverse transcription kit and stored at -20°C.

1.2.5 Quantitative real-time PCR (RT-PCR) amplification of the target gene, and preparation of RT-PCR reaction solution: 2× Master mix 10.0 (ul), Forward Primer 1.0 (ul), Reverse Primer 1.0 (ul), nuclease-free H₂O 1.0 (ul), Total per Reaction 18.0 (ul); The PCR reaction solution was divided into eight PCR tubes and 2ul cDNA prepared was added. The difference of gene expression was detected by fluorescence quantitative PCR.

1.2.6 Western Blot assay

(1) Cell collection: Cells were cultured to the density reached 80%, cells were scraped with a plastic scraper and collected in a centrifuge tube. (2) Protein extraction: wash twice with PBS and discard as much as possible residual PBS. The cells were resuspended with an appropriate volume of RIPA lysate, and then the cells were cleaved with ultrasonic apparatus for 10sec. Pyrolysis liquid centrifuged with 13000rpm at 4°C for 20min, the supernatant was transferred to a new tube, the protein content was determined by BCA method and diluted to the same concentration. The different treated samples with the same total protein content were mixed at 1: 3 and 4× Loading buffer, denaturated at 100°C for 5min, and stored at -20°C. (3) Gel preparation and electrophoresis: SDS-polyacrylamide gel electrophoresis was prepared. The concentrated gel was compressed at 60V, and the separation gel was separated at 120V for 1.5~2h. (4) Film transfer: after electrophoresis, remove and cut the glue, cut the film of the appropriate size according to the size, one layer of filter paper on each side, glue and film in the middle, glue in the negative electrode, film in the positive electrode, using full wet film transfer, constant current 0.25A to 1.5h~2.5h. (5) Red dyeing and sealing: the membrane was immersed in red dyeing solution, dyed for 1-2min, washed with distilled water, labeled protein, cut off the target strip, washed with PBST for 5min, and sealed with 5% skim milk powder at 37°C for 1h. (6) Antibody incubation: discard the blocking solution, dilute the primary antibody in the blocking solution, incubate at room temperature for

1~2h, or incubate overnight at 4°C; PBST was purified for 10min×5, the secondary antibody was diluted with the blocking solution and incubated in a shaker at room temperature for 1h. After the reaction, the secondary antibody was discarded and washed with PBST for 10min×5. (7) X-ray film is developed in a darkroom.

3 the results

3.1 Effect of 640nm red light on TGF-β and COL-I gene expression in fibroblasts

The fusion curves of GAPDH, TGF-β, COL, SAM, FN and Vim were credible, indicating that the amplification of target gene by primers was normal. Previous experimental results showed that there was significant cytotoxic effect of 640nm red light irradiation for 120min, so 30min and 60min irradiation intensities were selected for qPCR detection.

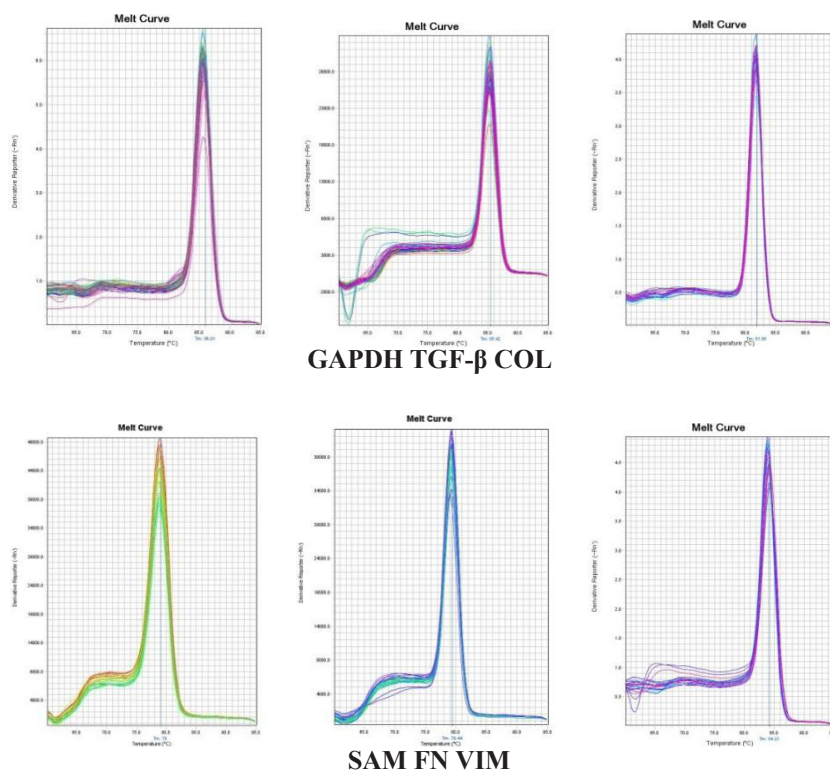


Figure 3-1. Fusion curves of TGF-β, Col-I; FN, SAM and VIM target genes

TGF-β gene expression was the most active in the control group after 24 hours of red light irradiation, and the mRNA expression of TGF-β was gradually down-regulated with irradiation time. TGF-β gene expression was gradually up-regulated in the 640nm red light irradiation group, and reached at the maximum level at 48h. Among them, 60min irradiation intensity had the most significant upregulation effect on TGF-β gene expression.

Compared with the control group, the 30min irradiation intensity increased the expression of Col-I at 24h, and down-regulated Col-I expression level after 48h. The 60min radiation intensity down-regulated the expression of Col-I at 48h, but significantly up-regulated the expression at 72h.

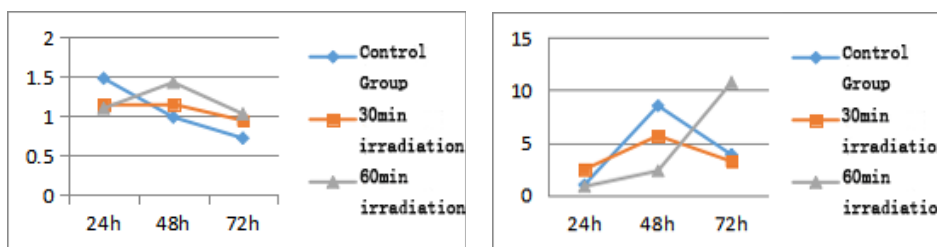


Figure 3-2 Effect of red light irradiation on TGF-β(left) and Col(right) gene expression in fibroblasts

3.2 Effect of 640nm red light on extracellular matrix

At the same time, the mRNA expression levels of different extracellular matrix were detected. The results showed that the expressions of SAM, Vim and FN genes were down-regulated in the different intensity of red light irradiation groups, and there was no difference of genes expression between the red light irradiation groups and the control group after 72h.

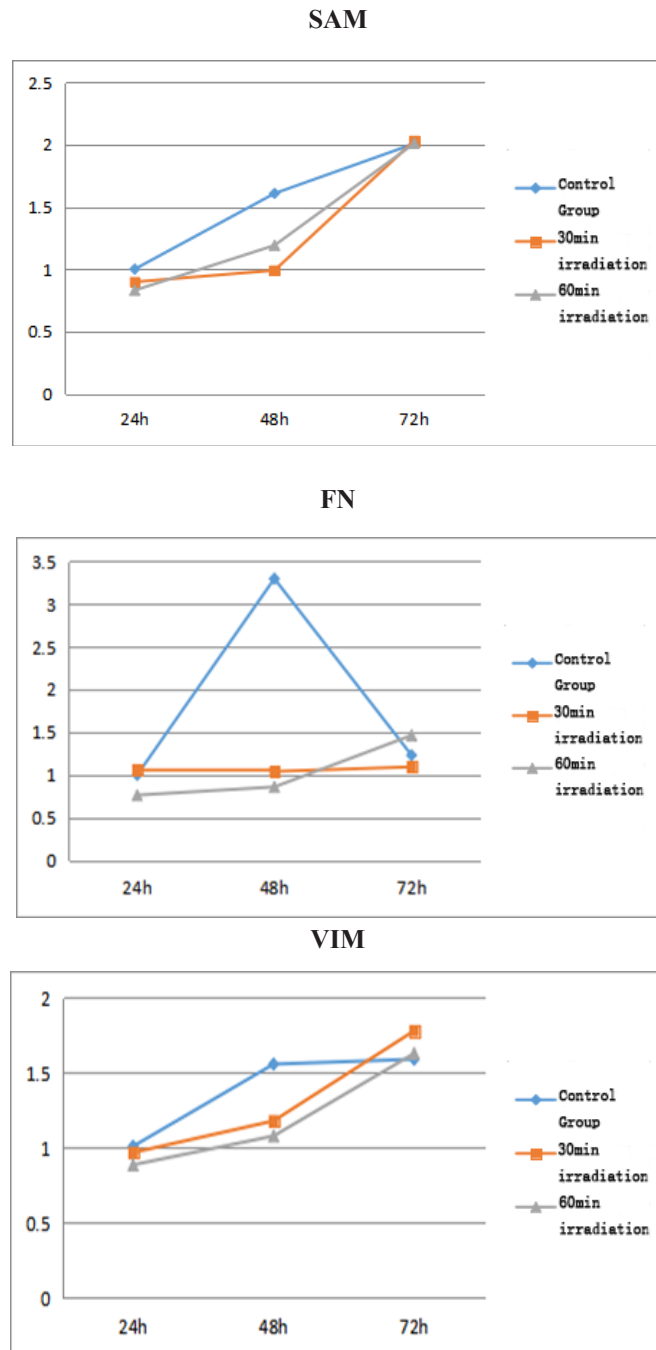


Figure 3-3 Effect of red light irradiation on SAM, FN and VIM gene expression in fibroblasts

3.3 Effect of 640nm red light on MAPK signaling pathway

MAPK is involved in multiple signaling pathways such as cell differentiation, proliferation and apoptosis. Regulation of three key proteins mediated by MAPK signaling pathway mainly includes ERK-mediated cell proliferation, JNK and p38 mediated inflammatory response under stress conditions, cell apoptosis and

immunomodulation processes. 60min 640nm red light irradiation enhanced the phosphorylation level of P42, had no significant effect on the phosphorylation level of JNK protein, and significantly inhibited the phosphorylation level of P38.

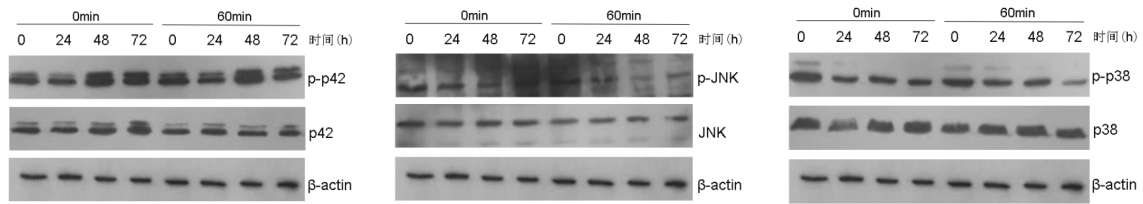


Figure 3-4 Effect of red light irradiation on MAPK signaling pathway

3.4 Influence of ERK on MAPK signaling pathway regulated by 640nm red light

To further investigate whether the increase of ERK signaling pathway induced by 640nm red light promotes fibroblast proliferation. In this study, ERK signaling pathway inhibitors were used to intervene. ERK inhibitors inhibited P42 phosphorylation, while ERK inhibitors and JNK inhibitors did not..

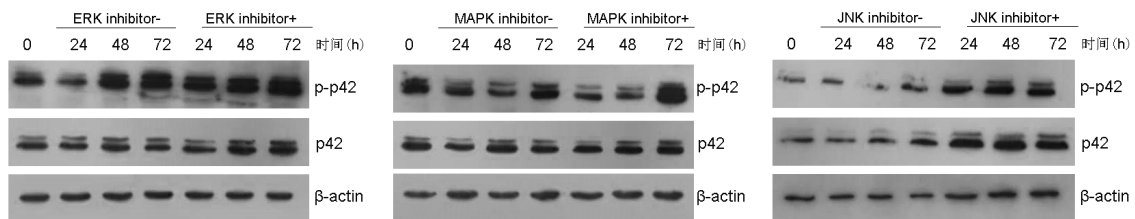


Figure 3-5 Influence of ERK on MAPK signaling pathway regulated by red light irradiation

3.5 Influence of JNK on MAPK signaling pathway regulated by 640nm red light

With the growth of cells, the phosphorylation level of JNK protein was not significantly affected by 640nm red light irradiation. Meanwhile, the JNK signaling pathway inhibitors did not affect the protein expression of the JNK signaling pathway. 640nm red light irradiation May not activate the JNK signaling pathway, which not affect the MAPK signaling pathway through the JNK pathway.

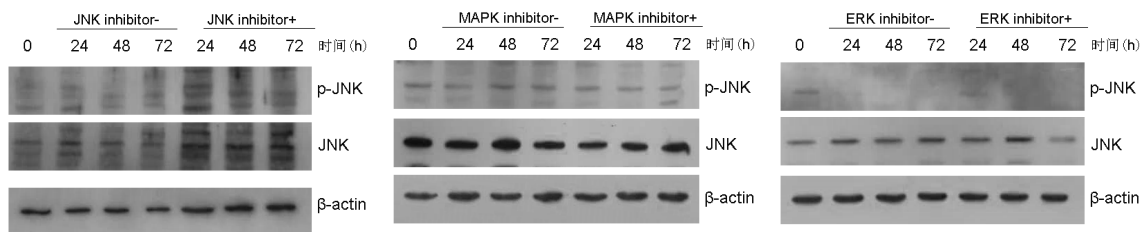


Figure 3-6 Influence of JNK on MAPK signaling pathway regulated by red light irradiation

3.6 Influence of P38 on MAPK signaling pathway regulated by 640nm red light

Phosphorylation of P38 was inhibited in the control group and the 60min irradiation group, and the 60min irradiation group significantly inhibited the activity of phosphorylated P38. Compared with the control group, P38 inhibitors upregulated the phosphorylation level of P38, while ERK inhibitors and JNK inhibitors did not. 640nm red light irradiation was also played a key role by affecting the P38 pathway of MAPK.

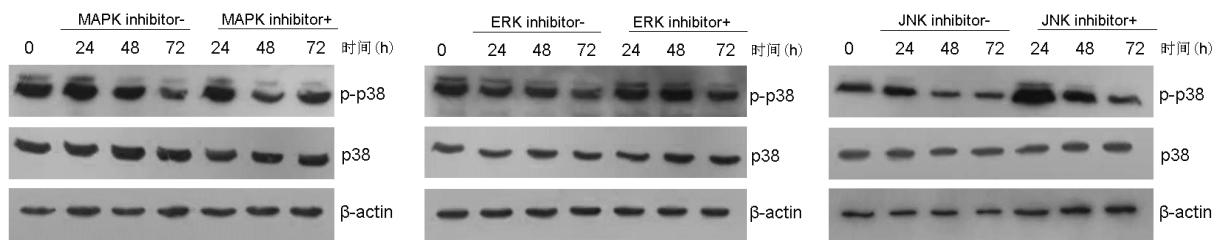


Figure 3-6 Influence of P38 on MAPK signaling pathway regulated by red light irradiation

4 discuss

Stretch marks are caused by a decrease in the number of fibroblasts or collagen production. TGF- β is a major regulator of collagen synthesis in fibroblasts^[30]. On the one hand, it regulates the transcription, translation and secretion levels of collagen in fibroblasts, and on the other hand, it can inhibit collagen degradation and accelerate collagen deposition by selectively inhibiting collagenase activation and expression^[30]. TGF- β also regulates the expression and secretion levels of other extracellular matrix, such as hyaluronic acid, fibro connection and receptors, laminin, proteoglycan and so on^[31]. Promoting the growth and proliferation of fibroblasts and contraction of collagen fibers are the main ways to treat stretch marks. At present, red light therapy is widely used in anti-inflammatory, accelerating tissue repair, promoting fracture healing, reducing scar and other fields^[32]. 640nm is a small wavelength of red light, which is mainly used in the field of skin therapy. However, the therapeutic effect of 640nm red light on stretch marks is still unclear, and the specific regulatory mechanism is rarely studied.

In this study, fibroblasts were irradiated with different intensities of red light to promote the proliferation of cultured fibroblasts in vitro and induce the secretion of TGF- β , and the irradiation intensity of 60min had the most obvious regulation effect on TGF- β gene expression. TGF- β is the main regulatory factor of human skin procollagen production, which can promote the proliferation and division of fibroblasts cultured in vitro and the synthesis of collagen^[33]. Red light irradiation at 640nm can significantly up-regulate the mRNA expression of collagen in human fibroblasts. There was no significant difference in the SAM, Vim and FN genes in extracellular matrix gene expression.

MAPK signaling pathway is related to a variety of cell functions, and can be involved in a variety of physiological processes such as cell movement, apoptosis, differentiation, growth and proliferation^[34]. This pathway mainly contains three key protein regulatory roles: ERK mediated cell proliferation, JNK and p38 mediated inflammatory response under stress conditions, cell apoptosis and immune regulation. In order to further explore the role of MAPK signaling pathway in the regulation of TGF- β secretion by 640nm red light irradiation, western blotting detected the protein expression differences of three major signaling pathways of MAPK signaling pathway, namely JNK, ERK, and P38. Compared with the control group, 640nm red light plays a significant regulatory role in ERK and P38 signaling pathways, which mainly promoted the phosphorylation level of P42 protein and inhibited the phosphorylation level of P38 protein, thereby regulating the MAPK signaling pathway and further regulating the expression of downstream target genes. ERK inhibitors can down-regulate the phosphorylation level of P42 protein induced by red light irradiation at 640nm, while JNK inhibitors and MAPK inhibitors do not have this effect. The results indicate that red light irradiation at 640nm promotes the proliferation of fibroblasts by affecting the ERK pathway. Red light irradiation at 640nm had no effect on the expression of JNK pathway proteins, nor did ERK, JNK and MAPK inhibitors. Red light irradiation at 640nm did not regulate MAPK through JNK signaling pathway. Red light irradiation at 640nm significantly inhibited the phosphorylation level of P38 protein, while P38 inhibitors reversed the down-regulation effect, while ERK inhibitors and JNK inhibitors could not play this role. The results showed that red light irradiation at 640nm regulates the downstream pathways by affecting the P38 pathway of MAPK, thereby regulating the expression of collagen in fibroblasts. Three signaling pathway has its own characteristics. Different or completely opposite biological effects can

be produced by the coordination and integration of signals between different subclasses of stimulus factors such as cell culture time and red light irradiation intensity. Therefore. Further study still needs to explore parallel signaling pathways between mutual coordination and regulation mechanism.

In conclusion, this study found that 640 nm red light irradiation therapy was time- and dose dependence. After 48-72h of 60min irradiation, irradiation group significantly promoted the proliferation of human fibroblasts and increased mRNA level of TGF- β . 640 nm red light promote the synthesis of collagen by increasing cell proliferation and TGF- β gene expression, which further to improve the repair of skin stretch marks. 60min red light irradiation promotes the proliferation of fibroblasts by promoting the phosphorylation level of ERK protein of the MAPK family molecule, and further promotes the gene expression and secretion of collagen. 60min red light irradiation inhibited the P38 signaling pathway and reduced the inflammatory response of fibroblasts, thus promoting the proliferation and differentiation of fibroblasts. The 60min red light can promote the expression of collagen in fibroblasts by regulating the MAPK signaling pathway, which is expected to be a noninvasive and effective treatment for stretch marks repair.

Reference

1. Scott, L.J., Delafloxacin: A Review in Acute Bacterial Skin and Skin Structure Infections. *Drugs*, 2020. 80(12): p. 1247-1258.
2. Kanaki, T., E. Makrantonaki, and C.C. Zouboulis, Biomarkers of skin aging. *Rev Endocr Metab Disord*, 2016. 17(3): p. 433-442.
3. Ud-Din, S., D. McGeorge, and A. Bayat, Topical management of striae distensae (stretch marks): prevention and therapy of striae rubrae and albae. *J Eur Acad Dermatol Venereol*, 2016. 30(2): p. 211-22.
4. Trelles, M.A., J.L. Levy, and I. Ghersetich, Effects achieved on stretch marks by a nonfractional broadband infrared light system treatment. *Aesthetic Plast Surg*, 2008. 32(3): p. 523-30.
5. Moore, J., G. Kelsberg, and S. Safranek, Clinical Inquiry: Do any topical agents help prevent or reduce stretch marks? *J Fam Pract*, 2012. 61(12): p. 757-8.
6. McDaniel, D.H., Laser therapy of stretch marks. *Dermatol Clin*, 2002. 20(1): p. 67-76, viii.
7. Wolak, K. and R. Gruskiewicz-Majczak, Development of a combination therapy with silanols complexed with boron citrate and ablative-fractional laser for treatment of wrinkles and stretch marks. *J Dermatolog Treat*, 2020: p. 1-7.
8. Ried, A., et al., Distribution of excitation energy among photosystem I and photosystem II in red algae. I. Action spectra of light reactions I and II. *Biochim Biophys Acta*, 1977. 459(2): p. 175-86.
9. Falcone, D., et al., Effects of red light on inflammation and skin barrier recovery following acute perturbation. Pilot study results in healthy human subjects. *Photodermatol Photoimmunol Photomed*, 2019. 35(4): p. 275-276.
10. Kim, Y.J., et al., A Protective Mechanism of Visible Red Light in Normal Human Dermal Fibroblasts: Enhancement of GADD45A-Mediated DNA Repair Activity. *J Invest Dermatol*, 2017. 137(2): p. 466-474.
11. Nunez-Alvarez, C. and N.N. Osborne, Enhancement of corneal epithelium cell survival, proliferation and migration by red light: Relevance to corneal wound healing. *Exp Eye Res*, 2019. 180: p. 231-241.
12. Kurtti, A., et al., Light emitting diode-red light for reduction of post-surgical scarring: Results from a dose-ranging, split-face, randomized controlled trial. *J Biophotonics*, 2021: p. e2747.
13. Mamalis, A., et al., High fluence light emitting diode-generated red light modulates characteristics associated with skin fibrosis. *J Biophotonics*, 2016. 9(11-12): p. 1167-1179.
14. Aldahan, A.S., et al., Laser and Light Treatments for Striae Distensae: A Comprehensive Review of the Literature. *Am J Clin Dermatol*, 2016. 17(3): p. 239-56.
15. Pietrusinski, M., et al., Selected genes polymorphisms and the risk of non-syndromic striae. A case-control study in

the Polish population. *J Eur Acad Dermatol Venereol*, 2019. 33(8): p. e286-e288.

16. Schuck, D.C., et al., Unraveling the molecular and cellular mechanisms of stretch marks. *J Cosmet Dermatol*, 2020. 19(1): p. 190-198.
17. Feng, Y., et al., Targeted apoptosis of myofibroblasts by elesclomol inhibits hypertrophic scar formation. *EBio-Medicine*, 2020. 54: p. 102715.
18. Wilson, S.E., Corneal myofibroblasts and fibrosis. *Exp Eye Res*, 2020. 201: p. 108272.
19. Sasabe, R., et al., Effects of joint immobilization on changes in myofibroblasts and collagen in the rat knee contracture model. *J Orthop Res*, 2017. 35(9): p. 1998-2006.
20. Hardy, K.M., et al., FGF signalling through RAS/MAPK and PI3K pathways regulates cell movement and gene expression in the chicken primitive streak without affecting E-cadherin expression. *BMC Dev Biol*, 2011. 11: p. 20.
21. Liu, Z.F., et al., Heat stress prevents lipopolysaccharide-induced apoptosis in pulmonary microvascular endothelial cells by blocking calpain/p38 MAPK signalling. *Apoptosis*, 2016. 21(8): p. 896-904.
22. Frank, S.B., et al., Human prostate luminal cell differentiation requires NOTCH3 induction by p38-MAPK and MYC. *J Cell Sci*, 2017. 130(11): p. 1952-1964.
23. Guo, Y.J., et al., ERK/MAPK signalling pathway and tumorigenesis. *Exp Ther Med*, 2020. 19(3): p. 1997-2007.
24. Kang, K. and Y. Wang, Sevoflurane Inhibits Proliferation and Invasion of Human Ovarian Cancer Cells by Regulating JNK and p38 MAPK Signaling Pathway. *Drug Des Devel Ther*, 2019. 13: p. 4451-4460.
25. Li, Q., et al., Blocking MAPK/ERK pathway sensitizes hepatocellular carcinoma cells to temozolomide via down-regulating MGMT expression. *Ann Transl Med*, 2020. 8(20): p. 1305.
26. Wang, J.L., et al., Oleanolic acid inhibits mouse spinal cord injury through suppressing inflammation and apoptosis via the blockage of p38 and JNK MAPKs. *Biomed Pharmacother*, 2020. 123: p. 109752.
27. Gao, J., et al., Diptoinonesin G promotes ERK-mediated nuclear translocation of p-STAT1 (Ser727) and cell differentiation in AML cells. *Cell Death Dis*, 2017. 8(5): p. e2765.
28. Maurice, D., et al., ERK Signaling Controls Innate-like CD8(+) T Cell Differentiation via the ELK4 (SAP-1) and ELK1 Transcription Factors. *J Immunol*, 2018. 201(6): p. 1681-1691.
29. Poddar, R., et al., Role of AMPA receptors in homocysteine-NMDA receptor-induced crosstalk between ERK and p38 MAPK. *J Neurochem*, 2017. 142(4): p. 560-573.
30. Teodorescu, P., et al., Transforming growth factor beta-mediated micromechanics modulates disease progression in primary myelofibrosis. *J Cell Mol Med*, 2020. 24(19): p. 11100-11110.
31. Juhl, P., et al., Dermal fibroblasts have different extracellular matrix profiles induced by TGF-beta, PDGF and IL-6 in a model for skin fibrosis. *Sci Rep*, 2020. 10(1): p. 17300.
32. Mamalis, A., et al., MicroRNA expression analysis of human skin fibroblasts treated with high-fluence light-emitting diode-red light. *J Biophotonics*, 2019. 12(5): p. e201800207.
33. Walraven, M., R.H. Beelen, and M.M. Ulrich, Transforming growth factor-beta (TGF-beta) signaling in healthy human fetal skin: a descriptive study. *J Dermatol Sci*, 2015. 78(2): p. 117-24.
34. Lu, M., Y. Wang, and X. Zhan, The MAPK Pathway-Based Drug Therapeutic Targets in Pituitary Adenomas. *Front Endocrinol (Lausanne)*, 2019. 10: p. 330.



Pisco Med Publishing

Under COVID-19 Stress, What We Have Done, How We Are Doing, and What Shall We Do?

Shun Huang, M.D. Ph.

Associate chief physician of Anesthesiology department, Beijing Hospital, National Center of Gerontology; Institute of Geriatric Medicine, Chinese Academy of Medical Sciences, P.R. China. 100730, E-mail: huangshunsleet@126.com

Abstract: From the end of 2019 up to now, novel coronavirus (COVID-19) has swept the globe, bearing down menacingly, and generating massive burden not only on government and hospital, but also on almost every single person, especially medical workers. We are anesthesiologists, surgeons, and nurses in Beijing Hospital, witnesses of this cruel battle. I'd like to describe what happened in our real life in the past few months, how dose the epidemic situation change our lives and work, and what will we do in the future.

KEYWORD COVID-19; Stess; Medical workers

1. The Past Can't Be Traced

1.1 Expedition

Explosive news broke the joyous circumstances of the Chinese spring festival, City Wuhan, Hubei Province, the severely COVID-19 afflicted area, was lock down since January 23rd, 2020. We realized the aggravation of the situation and canceled our scheduled tours, visits and parties one after another. We stayed at home all day except when procurement or on duty. We focused on the affair development and waited for the enlist of hospital at any time.

On January 26th, 2020, the second day of the Chinese new year, the first medical team of our hospital rescuing Hubei Province set out, and Jie zhai, supervisor nurse of our surgical anesthesiology department, was on the list of 20 fighters. When ambiguous future and life-threatening danger ahead, it was rather hard to bid farewell with aging parents, callow children and familiar colleagues. Thousands of words about taking care and being health turned into four lines of hottish tears. At that moment, we are not only someone's wife/husband, someone's mother or daughter/father or son, but also medical workers bearing heavy responsibilities. At that moment, we felt we are more than who we are. We are the bravest warriors and the toughest soldiers to defeat raging virus.

1.2 Torture

The following days we trapped at home together with our family, masks sold out, vegetables scarced, prices of daily use material went up, no elective surgery submmited, and morning lectures canceled. Every body immersed in a tense, worry, and anxiety mood, ceaselessly washing, sterilizing, and refreshing the news and Wechat, searching for messages from the front line. Director of our department MingZhang Zuo set about to formulate a protection guideline of anesthesiologist airway management with other airway experts, aiming to protect medical staff and decrease spread of the disease. The second medical team of 123 fighters followed up on Feburary 7th, 2020, with a bunch of protection equipments. This time our venerable dean JianYe Wang was in command by himself. Before left, he made an oath that all his team members must go back safe and sound.

What happened in Wuhan was dreadful. The raging virus took away many lives including medical workers although being taken good care, paralyzed medical institutions both public and private, and caused enormous loss and anguish on broad masses of people. Fortunately, government strictly controlled the chaotic situation, increasing publicity input and reallocating medical resources, and then the sick city gradually recovered under unsurpassed efforts of whole national people. Rushing into rescue in a planned way, such as adequate and in time equipment supply, and the mobile cabin hospital built-up in short term, all of these healed the wounds left by the severe infectious disease. Our third medical team of 8 fighters hurried off for rescue on February 22th, 2020, they are all males, strong and passionate, injecting fresh blood for the battle once again. On April 8th, 2020, after experiencing disaster and salvation, the sleeping city Wuhan restart at last^[1].

1.3 Triumphant

After extremely hard and bitter work, our heroes returned home in triumph on April 6th, 2020, passed through fourteen days' quarantine, on April 21st, 2020, a royal welcome ceremony was held grandly. Staff hugged their long lost friends, ardent father hold up his lovely son, husband kissed his long-separated wife, and a young doctor made a successful proposal with a beautiful hero nurse. We are brave when we have to, we present strength in face of danger, and we enjoy the victorious joy, yes, we made it at last. All together 151 heroes went home safely.

Although we have submitted a satisfactory paper, we all don't like to mention the period of time--there are too much pain, sorrow, excitement and tears in the historical moment.

2. Live In The Moment

2.1 Revive

The past can be hurt, and we can either run from it or learn from it. Early in late February, our hospital have carried out novel coronavirus nucleic acid test. We could screen patients by ourselves, discriminating suspected cases and admitting emergency or selective surgical patients. Wholely March, April and May, rate of utilization of hospital beds increased gradually from 0 to 70%. More and more suspensory operations have been done. We were used to monitoring temperature and supplying past 14 days' journey track whenever entering public places, and wearing surgical mask whenever leaving home^[2].

Although out-city trip was not allowed, since there was no new case of COVID-19 in Beijing continuously over 50 days, some of us began to get together having a quick simple meal, our children went back to school successively, and deliveryman could delivery cargo at our front door again. Hospital called upon us to roll up sleeves working harder, and the postponed college and high-school entrance examinations had been scheduled, and all walks of life were unfreezed and welcome their delayed spring. The situation looked good. It seems like that the epidemic disease has been away from us.

2.2 Blockbuster

Suddenly a big news broked the hard-won calmness, on June 11th, 2020, a 52-year-old male patient in Xicheng district was identified as COVID-19. Every person's just relaxed emotion became tense again. But this time, we had suitable psychological anticipation and previously aquired experience. This was a challenge also an opportunity to try our hands at the epidemic disease, knowing if we were prepared well enough.

Rapidly, Beijing set up first-order response, government, center for disease control and prevention. Hospitals, schools, and subdistrict offices went into action. Our children went back home again after transient school-open. Epidemiological investigation quickly locked the contaminating resource — Newfoundland market in Fengtai district. Thanks to the Wechat and Alipay big data, thousands of people who had ever been to the market in ten days were traced and quarantined at home instantly.

On June 14th, 2020, our hospital imminently deployed A04 quarantine inpatient ward to receive and cure suspected patients. Then the whole city started a craze of nucleic acid test. On June 20th, 2020, all our staffs conducted the test ourselves, insuring safe to coming patients, and we allocated 200 staff to do the test for community and school. Dr. Jie bao and Dr. RuiFang Jia of our department are members of them.

During that time, one of our emergency patients who was pregnant requiring for cesarean section was identified suspended case. Two days after surgery, intimate-contact staffs were quarantined at C02 inpatient area, centrally collective management, Dr. JingJing Zhang and Dr. JunFeng Li, two anesthesiologists on duty that night, got a full time rest for seven days in separated ward, until the patient was excluded from the suspension.

2.3 Appease

All of the control and prevention managements underwent nervously and orderly. We paid close attention to every high-risk and middle-risk street, road and district everyday. People living in the high-risk area weren't allowed to enter our hospital, and staff living in the middle-risk area must supply lately nucleic acid test with negative result before entering work area. It seemed like that all we should do have already done.

One month later, finally, we got over the toughest time. After many day, Beijing had no newfound cases any more. Students took part in college and high school entrance examination as scheduled. Again we submitted a satisfactory paper, what we have to say, we have indeed learned a lot from the past^[3].

3. The Future Can Be Expected

3.1 Hope

Things didn't always go the way we planned, after denial, angry, bargain and sadness, it was time to accept the fact that we will coexist with novel coronavirus for a while before defeating it.

At the first stage of the battle, we were unprepared, flustered, and bewildered; on the second round, we recognized the enemy, grasped some of its characteristic, and could handle it whenever it arises; then the next step should be our home court, we should think ahead, go into action, and be committed to eliminating the raging virus from the very beginning. Research and development of Vaccines have been carried out, many treatment methods have been tried and introduced into trials.

3.2 Change

The epidemic situation has changed our life invisibly. We spend much more time with our family and reinforce the protection to more higher level ; we become patient teachers companying our children to study internet-classes; we practice defensive mechanism in face of unexpected accident; we introspect on ourselves and come across another leisured composed selfhood; we understand the meaning of life more thoroughly, making more efforts to live, to share and to give.

Professor Mingzhang Zuo's anesthesiologist protection guideline has been published in early February, being of massive referential value. Dr. Zhe Jia unexpectedly found a new high-salary job at this crisis time. I spent much of time to read articles about COVID-19, aspiring to discover thread of spider and trail of a horse. Dr. RuiFang Jia's son got into his favored middle school. Dr. Ning Yang gave birth to her second child, a little princess. Dr. Jie Bao will marry his fiancee in the near future. So many beautiful things are still continued. We have enough reasons to believe that the future is expected.

3.3 Vision

From biting cold winter to burning hot summer, we have experienced ordeal of vital importance, with gradually alleviating the daily life prevention equipments and increasing the empirical value of solutions. We will finally break the

chains of epidemic disease. Whatever happened, graduates of this year eventually said goodbye to the past, and would embrace their brand new future. More and more students aspire for being a good doctor, inspired by medical workers' sacred professional integrity, and having qualified successors is rather gratified for us.

Hoping one day medical recues have no country-border, and "one world one dream" will come true;

Hoping one day our children can breathe freely and laugh merrily, leading better lives cared by the best science;

Hoping one day when we look back our lives, we are satisfied with our noble character and gainly posture.

1. Yao, W., et al., Emergency tracheal intubation in 202 patients with COVID-19 in Wuhan, China: lessons learnt and international expert recommendations. *Br J Anaesth*, 2020. 125(1): p. e28-e37.
2. Wu, J.T., K. Leung, and G.M. Leung, Nowcasting and forecasting the potential domestic and international spread of the 2019-nCoV outbreak originating in Wuhan, China: a modelling study. *Lancet*, 2020. 395(10225): p. 689-697.
3. Zuo, M.Z., et al., Expert Recommendations for Tracheal Intubation in Critically ill Patients with Noval Coronavirus Disease 2019. *Chin Med Sci J*, 2020. 35(2): p. 105-9.